Supporting Information

Ligand Tuning of Single-Site Manganese-based Catalytic Antioxidants with Dual Superoxide Dismutase and Catalase Activity

Michaela Grau, [a]Francesco Rigodanza,[b] Andrew J.P. White,[a] Antonio Sorarù,[b] Mauro Carraro,[b] Marcella Bonchio*,[b] and George J.P. Britovsek*.[a]

General Remarks

Synthetic manipulations of moisture- and oxygen-sensitive compounds were carried out under an inert-nitrogen atmosphere, on a vacuum line, using standard Schlenk and cannula techniques. Additionally, conventional nitrogen atmosphere glove boxes were used for the preparation of analytical and spectroscopic samples, as well as for the weighing and storage of air and moisture sensitive compounds.

Analytical Details

^{1}H, ^{19}F, ^{13}C, and 2D NMR spectra were recorded using AC-400 MHz, DRX-400 MHz and AM-500 MHz spectrometers. Variable temperature (VT) ^{1}H and ^{19}F NMR spectra were recorded using the DRX-400 MHz spectrometer. ^{1}H and ^{13}C NMR chemical shifts are indicated in parts per million (ppm) relative to the residual protio impurity of the deuterated solvent and ^{13}C NMR signal of the deuterated solvent, respectively. ^{13}C NMR spectra have been recorded with proton decoupling. ^{19}F NMR chemical shifts are referenced externally to $CFCl_3$ at 0 ppm. Coupling constants *J* are given in Hertz. The following abbreviations have been used to describe the multiplicities of the NMR signals: s (singlet), d (doublet), t (triplet), dd (double doublet), dt (double triplet), br (broad signal) and m (multiplet).

Mass spectra were recorded by Mr. J. Barton using either a VG Autospec or a VG Platform II spectrometer. Different methods such as electrospray (ESI), electron impact ionisation (EI) or liquid secondary ion mass spectrometry (LSIMS) were applied depending on the compound.

UV/Vis spectra were recorded in an acetonitrile solution using a Perkin-Elmer Lambda 20 or a Perkin-Elmer Lambda 2 spectrometer.

Cyclic voltammetry studies were performed using a PalmSens potentiostat equipped with a platinum disk working electrode, a platinum wire ancillary electrode and a $Ag/AgNO_3$ (0.01 M) in acetonitrile. The electrolyte was tetrabutylammonium hexafluorophosphate (0.1 M).

Infrared spectroscopy data were obtained directly from solid samples using a Perkin Elmer Spectrum 100 or a Nicolet 5700 FT-IR instrument a FT-IR spectrometer.

Elemental analyses were performed by Mr. S. Boyer at the London Metropolitan University.

X-ray diffraction analyses were carried out and solved by Dr. A. White at Imperial College London.

Head-space gas analysis was performed using a 7890A Agilent Technologies gas-chromatograph equipped with one 30 m long HP-MOLSIEVE column (0.32 mm diameter, 12 μm thickness) and one 30 m long HP-MOLSIEVE, (0.32 mm diameter and 20 μm thickness), and featuring FID, TCD and 5975C Agilent technologies MS detectors.

Solvents

All solvents used for air and moisture sensitive manipulations were stored in sealed glass ampoules under an atmosphere of nitrogen. Pentane and toluene were dried by passing through a cylinder containing commercially available Q-5 reactant (13 % w/w) copper(II) oxide on alumina and activated alumina (pellets, 3 mm) under nitrogen pressure. Diethyl ether and tetrahydrofuran were dried by prolonged reflux under a nitrogen atmosphere over sodium benzophenoneketyl. Dichloromethane and acetonitrile were refluxed over calcium hydride. All solvents were freshly distilled under nitrogen and degassed by three freeze-thaw cycles prior to use. All NMR solvents, CD_2Cl_2, $CDCl_3$, CD_3CN were degassed by three freeze-thaw cycles, dried over 4 Å molecular sieves and stored under nitrogen in sealed glass ampoules. Pyridine, methanol and dimethylsulfoxide were purchased absolute from Sigma Aldrich, degassed by three freeze-thaw cycles prior to use and stored under nitrogen in sealed glass ampoules.

Starting Materials and Reported Compounds

Unless specified otherwise, all commercially available starting materials and solvents were used without further purification. The following compounds were prepared by published procedures: 2-methylaminomethylpyridine,[1] *N*-methyl-(aminomethyl)pyridine ((NMe)2Py3, **1**),[2] *N*-tosyl-(aminomethyl)pyridine,[3] 2,6-diformylpyridine,[4] 2,6-bis[((2-pyridylmethyl)oxy)methyl]pyridine (O2Py3, **2**),[3] 2,6-bis[((2-pyridylmethyl)thio)methyl]pyridine (S2Py3, **3**),[3] 2,6-dimercaptomethylpyridine,[5, 6] 2,6-dichloromethylpyridine hydrochloride.[5, 7] *N*,*N*'-ditosyl-2,6-bis[(2-pyridylmethyl)amino)methyl]-pyridine ((NTosyl)2Py3, **1'**) has been described in the literature,[3] but here a different synthetic route was used:

2,6-Bis[(*N*-tosyl(2-pyridylmethyl)amino)methyl]pyridine, (NTosyl)2Py3**(1')**

2,6-dichloromethylpyridine hydrochloride (2.0 g, 9.4 mmol), *N*-tosyl-(aminomethyl)pyridine (4.9 g, 18.8 mmol) and potassium carbonate (5.2 g, 37.6 mmol) were suspended in abs. acetonitrile. The reaction mixture was stirred overnight at room temperature followed by 4 h stirring at 70 °C. After the mixture was cooled to room temperature, the solvent was removed and the residue taken up in dichloromethane and conc. aqueous sodium hydrogencarbonate. After separating the organic and aqueous layer, the aqueous phase was extracted three times with dichloromethane. The organic phase was dried over $MgSO_4$, filtered and the solvent removed, yielding the product as a beige solid (4.47 g, 76 %).

^{1}H NMR ($CDCl_3$, 400 MHz): δ (ppm) = 8.34 (d, J = 8.2 Hz, 2H, 6-Py*H*), 7.64 (d, J = 7.6 Hz, 4H, Ar*H*), 7.54 (t, J = 7.7 Hz, 2H, 4-Py*H*), 7.38 (t, J = 7.7 Hz, 1H, PyH_p), 7.31 (d, J = 7.9 Hz, 2H, 3-Py*H*), 7.22 (d, J = 7.9 Hz, 2H, Ar*H*), 7.08 (d, J = 7.4 Hz, 2H, PyH_m), 7.07 (t, J = 6.8 Hz, 2H, 5-Py*H*), 4.49 (s, 4H, 2 x NCH_2), 4.46 (s, 4H, 2 x NCH_2), 2.38 (s, 6H, 2 x CH_3). ^{13}C NMR ($CDCl_3$, 101 MHz): δ (ppm) = 156.5, 155.8, 148.7, 143.5, 137.1, 136.9, 129.7, 127.5, 122.9, 122.5, 121.3, 77.5, 77.2, 76.8, 53.9, 53.7, 21.6. ESI-MS: *m/z* = 650 $[M+Na]^+$, 628 $[M+H]^+$.

Metal Complexes:

[Mn(**1**)Cl_2]: The ligand **1**(239 mg, 0.69 mmol) was dried under vacuum for 2 h and dissolved in abs. THF (10 mL). Under inert atmosphere, the solution of the ligand was added to a suspension of [$MnCl_2(THF)_2$] (186 mg, 0.69 mmol)in abs. THF (10 mL). The light yellow reaction mixture was stirred overnight at room temperature. The solvent was removed under reduced pressure to a third of the volume. The complex was isolated by precipitation with pentane and dried under vacuum and was obtained as an off-white solid. Yield: 178 mg (55 %). *Crystals suitable for X-ray analysis were grown by slow diffusion from a dichloromethane solution layered with diethylether resulting in the presence of one dichloromethane in the unit cell.* LSIMS *m/z* = 437 $[(M\text{-}Cl)]^+$. Anal. Calcd. (found) for $C_{21}H_{25}Cl_2MnN_5$: %C 53.29 (53.01), %H 5.32 (5.02), %N 14.80 (14.65). UV/Vis (CH_3CN, 0.05 mM): λ_{max} in nm (ε in $M^{-1}cm^{-1}$): 266 (7000).

*General procedure to prepare manganese(II) bis(triflate) complexes [Mn(**L**)(OTf)$_2$]*

The relevant ligand **L** and 1.0 molar equivalent of [Mn(MeCN)$(OTf)_2$] were placed in different Schlenk flasks and dissolved in abs. tetrahydrofuran. After adding the solution of the ligand to the suspension of the metal precursor, the reaction mixture was stirred overnight at room temperature. The resulting solution was concentrated to one third of the initial volume. Diethyl ether was added to precipitate the product, which was dried under vacuum. If the complex already precipitated from the tetrahydrofuran solution during the reaction, the solvent was removed by filtration and the solid dried under vacuum.

[Mn(**1**)$(OTf)_2$]: Beige solid, 73 % yield. ^{19}F NMR (CD_3CN, 376 MHz, *broad singlet*): δ (ppm) = −65.90. LSIMS *m/z* = 551 $[M\text{-}OTf]^+$. Anal. Calcd. (found) for $C_{23}H_{25}F_6MnN_5O_6S_2$: %C 39.43 (39.59), %H 3.60 (3.46), %N 10.00 (9.93). UV/Vis (CH_3CN, 0.05 mM): λ_{max} in nm (ε in $M^{-1}cm^{-1}$): 264 (12000), 328 (1400). μ_{eff} (CD_3CN) = 6.02 BM.

[Mn(**2**)$(OTf)_2$]: White solid, 65 % yield. *Crystals suitable for X-ray analysis were grown by slow diffusion from a dichloromethane solution layered with diethylether. It is worth noting that the complex is poorly soluble in THF and CH_2Cl_2.* LSIMS *m/z* =

525 $[M\text{-}OTf]^+$. Anal. Calcd. (found) for $C_{21}H_{19}F_6MnN_3O_8S_2$: %C 37.40 (37.55), %H 2.84 (2.75), %N 6.23 (6.18). UV/Vis (CH_3CN, 0.05 mM): λ_{max} in nm (ε in $M^{-1}cm^{-1}$): 262 (13100), 208 (16900). μ_{eff} (CD_3CN) = 6.08 BM.

$[Mn(\mathbf{3})(OTf)_2]$: White solid, 71 % yield. ^{19}F NMR (CD_3CN, 376 MHz, *broad singlet*): δ (ppm) = −52.71. LSIMS *m/z* = 557 $[M\text{-}OTf]^+$. Anal. Calcd. (found) for $C_{21}H_{19}MnF_6N_3O_6S_4$: %C 35.70 (35.39), %H 2.71 (2.50), %N 5.95 (5.25). UV/Vis (CH_3CN, 0.05 mM): λ_{max} in nm (ε in $M^{-1}cm^{-1}$): 266 (10000). μ_{eff} (CD_3CN) = 5.90 BM.

$[Mn(\mathbf{1'})(OTf)_2]$: White solid, 74 % yield. LSIMS *m/z* = 831 $[M\text{-}OTf]^+$. Anal. Calcd. (found) for $C_{35}H_{33}F_6MnN_5O_{10}S_4$: %C 42.86 (42.78), %H 3.39 (3.30), %N 7.14 (7.08). UV/Vis (CH_3CN, 0.05 mM): λ_{max} in nm (ε in $M^{-1}cm^{-1}$): 264 (13000), 234 (26000). μ_{eff} (CD_3CN) = 5.76 BM.

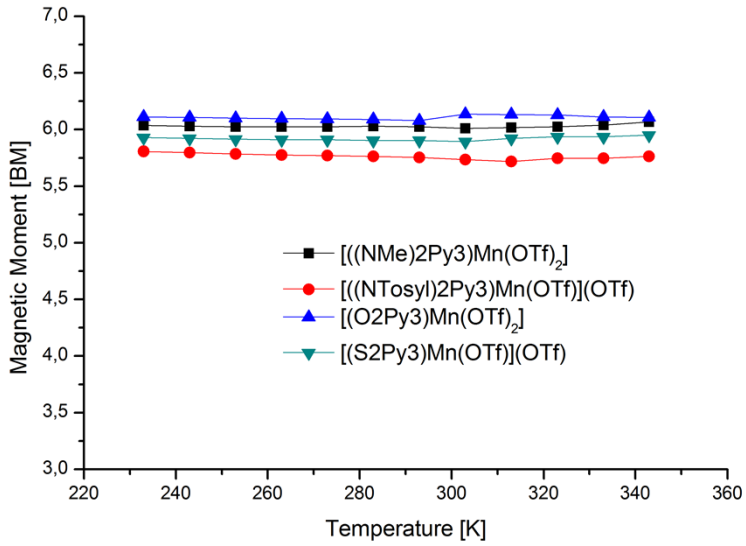

Figure S1: Effective magnetic moments of manganese(II) complexes [Mn(**1**)$(OTf)_2$], [Mn(**1'**)$(OTf)_2$], [Mn(**2**)$(OTf)_2$] and [Mn(**3**)$(OTf)_2$] in acetonitrile between 233 and 343 K.

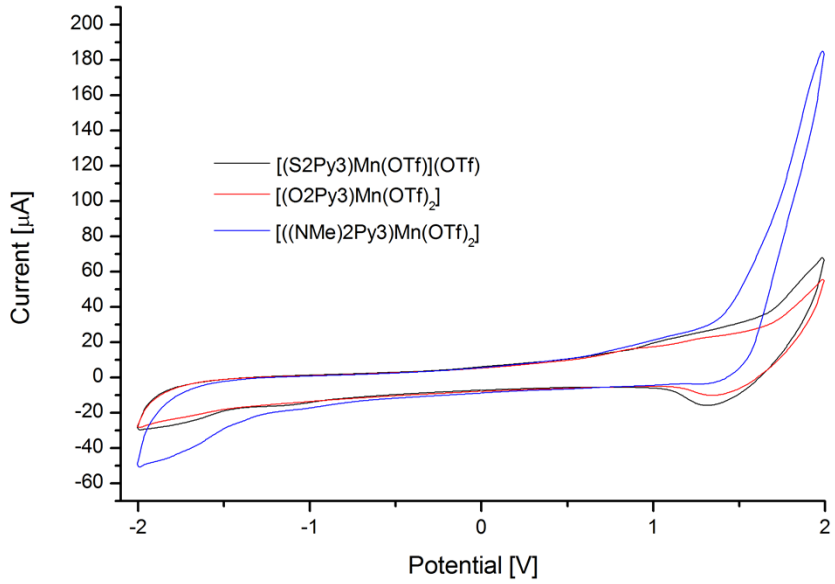

Figure S2: Cyclic voltammograms of manganese complexes [Mn(**1**)$(OTf)_2$],[Mn(**2**)$(OTf)_2$] and [Mn(**3**)$(OTf)_2$] in acetonitrile (5 mM) and tetrabutylammonium hexafluorophosphate (0.1 M) measured at 0.1 V/s *vs*. $Ag/AgNO_3$ (1 mM).

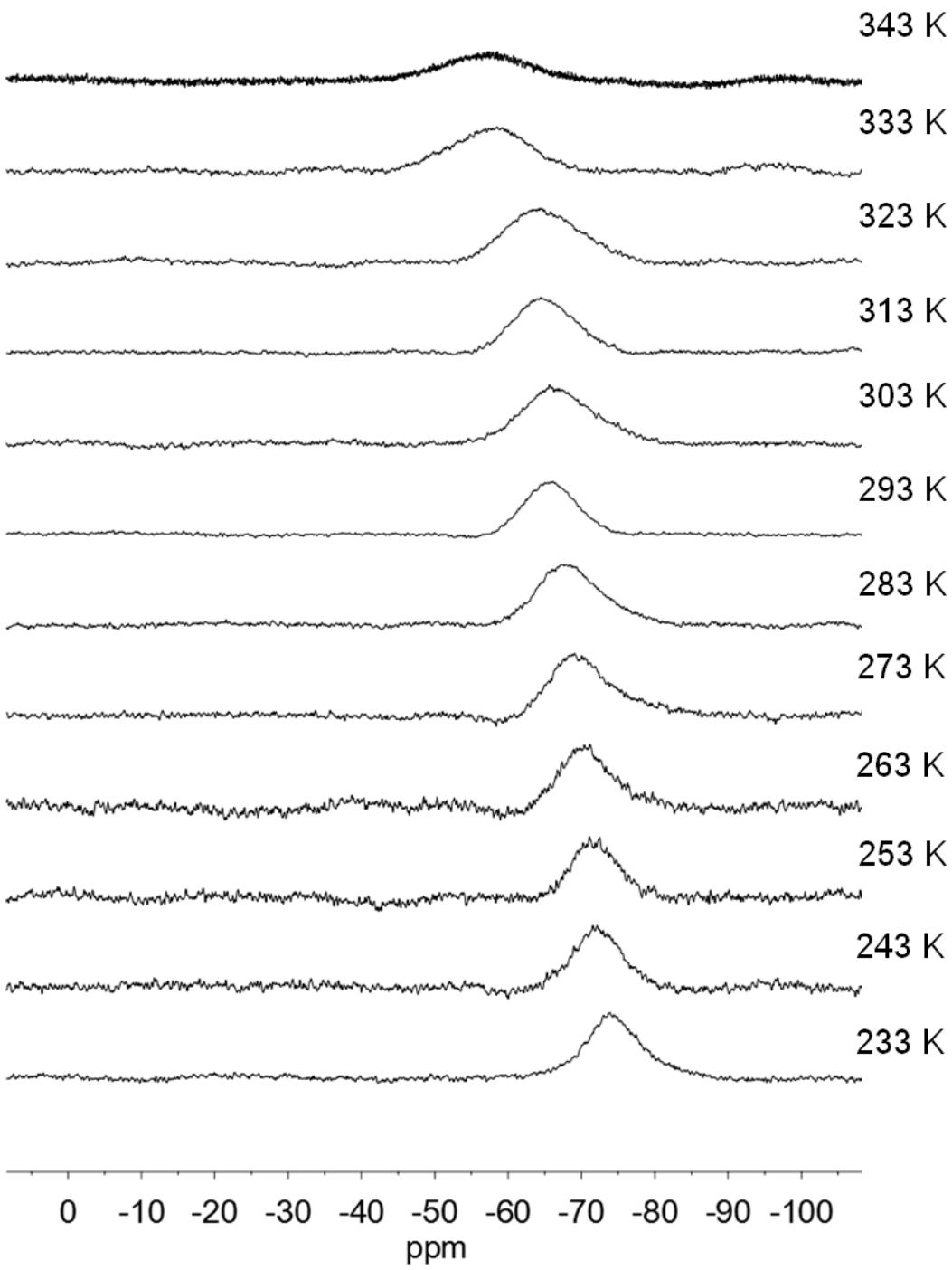

Figure S3: VT-^{19}F NMR spectra of [Mn(**1**)$(CD_3CN)_2$]$(OTf)_2$ in CD_3CN 233 to 343 K.

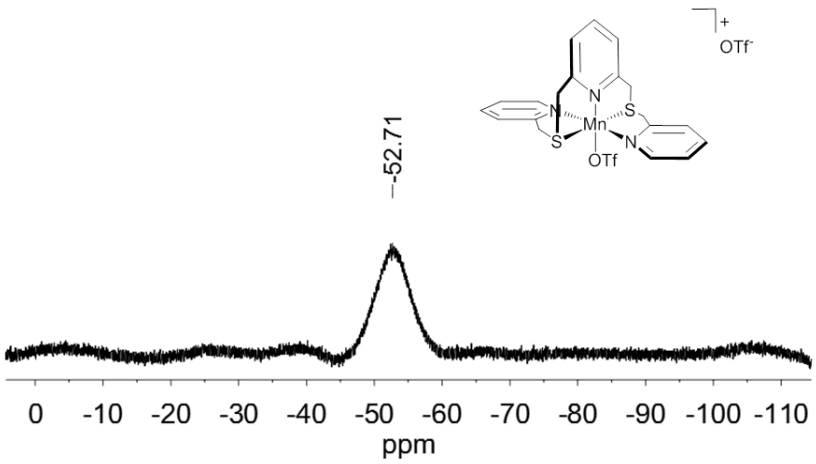

Figure S4. ^{19}F NMR spectrum of [Mn(**3**)$(CD_3CN)_2$]$(OTf)_2$ in CD_3CN at room temperature.

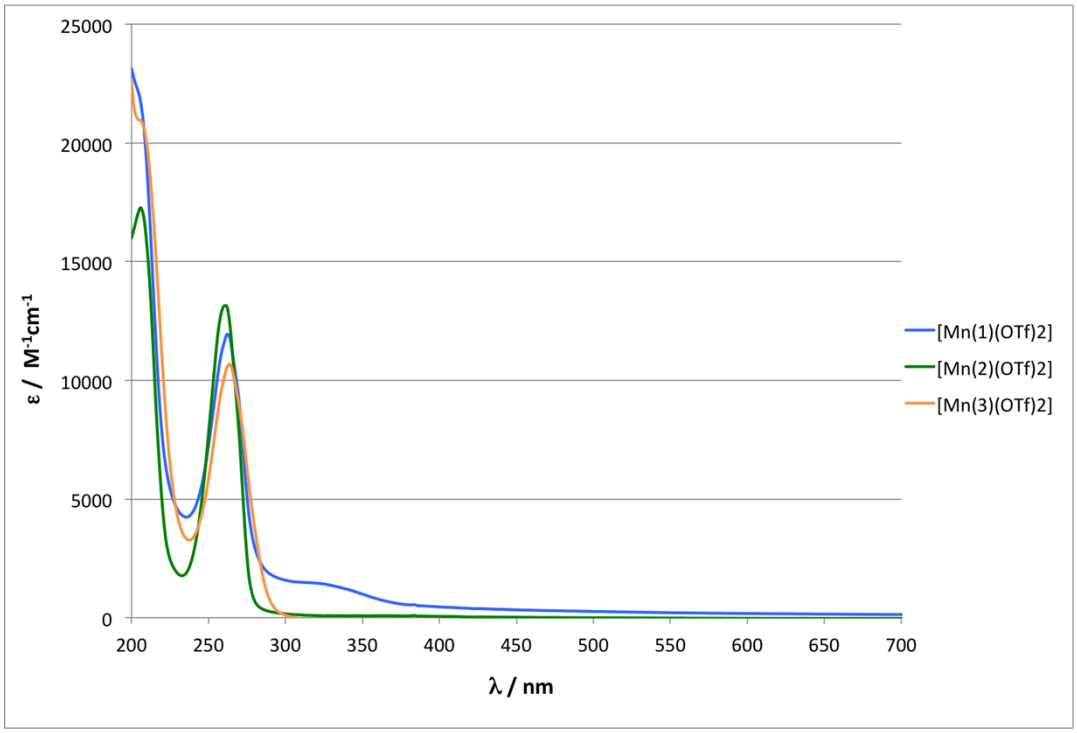

Figure S5a. UV-vis spectra of manganese(II) complexes [Mn(**1**)$(OTf)_2$] (blue), [Mn(**2**)$(OTf)_2$] (green) and [Mn(**3**)$(OTf)_2$] (orange) in CH_3CN at 298 K (c = 0.05 mM, 1 cm cuvette).

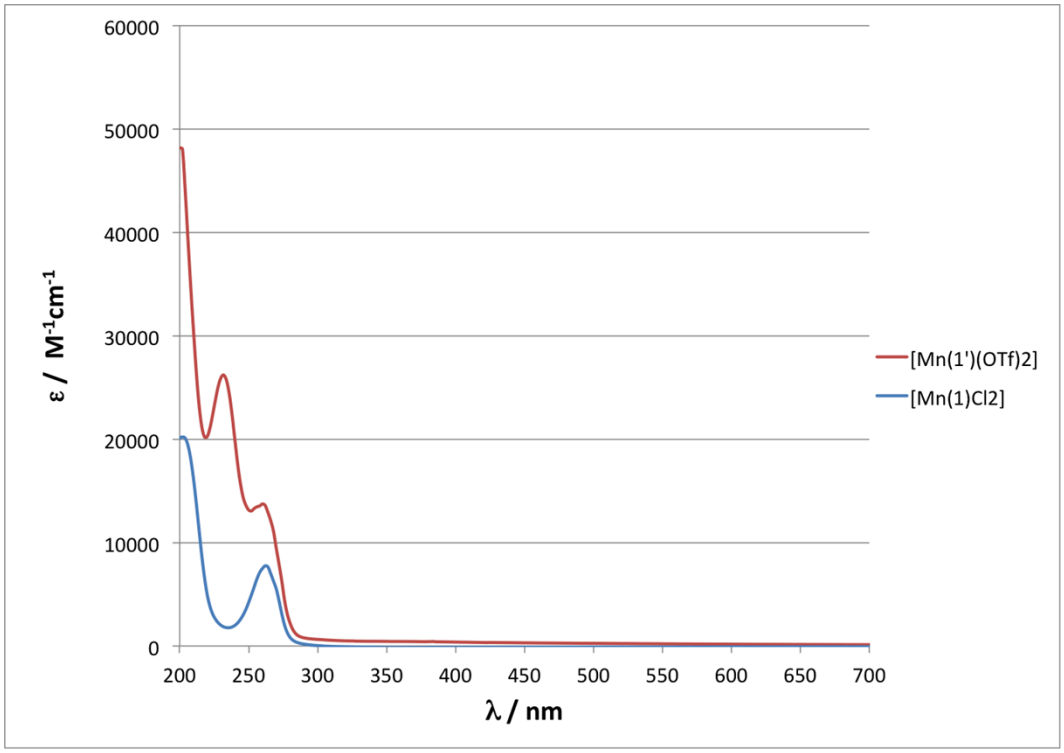

Figure S5b. UV-vis spectra of manganese(II) complexes [Mn(**1'**)$(OTf)_2$] (red) and [Mn(**1**)Cl_2] (blue) in CH_3CN at 298 K (c = 0.05 mM, 1 cm cuvette).

Catalytic Screening

H_2O_2 dismutation by Mn-based single site catalysts:

To a solution of H_2O_2 (33 mM) in CH_3CN (12 ml) the selected Mn complex (30-90 μM) was added to start the dismutation reaction. The reactor was maintained at 25 ± 0.2 °C by a thermostat, and the progress of reaction was determined by monitoring the concentration of molecular oxygen generated from hydrogen peroxide into a constant nitrogen flux of 5 ml/min. The amount of O_2 was determined by GC sampling and/or by continuous detection of pressure variation, through a pressure transducer equipped vial cap. Initial rates were calculated by linear regression of data within 5% H_2O_2 conversion. Kinetic runs were performed in triplicate, errors were estimated to be in the range of 1-2% (Fig. S5, Table S1). To investigate the catalyst fate, FT-IR spectra of [Mn(**2**)$(OTf)_2$] were analyzed before and after reaction, upon solvent removal (Fig. S7). The effect of acid/base additives was screened in the presence of 10 μl HCl (0.1 M), or 10 μl NaOH (1M).

Catalase-like activity by [Mn(**3**)$(OTf)_2$] (60 μM) was observed in water (12 ml, borate buffer 0.05 M, pH 9.2), in the presence of H_2O_2 (33 mM) and upon addition of imidazole (600 μM). Control experiments performed either without the Mn-based catalyst or imidazole, confirmed that no oxygen evolution is detected from the borate buffer solution in presence of H_2O_2.

Screening of Mn single site catalysts as SOD-mimics

Mn induced SOD-like activity was measured by spectrophotometric analysis of the inhibition of the superoxide-dependent reduction of the NBT chromophore. The superoxide radical anions generated by the xanthine/xanthine oxidase system, in phosphate buffer at pH 7.4, were detected measuring the reduction of NBT to blue formazan at 550 nm. In all experiments, the reaction mixture was prepared with 50 μM xanthine, 100 μM NBT, 50 mM phosphate buffer (pH 7,40) and xanthine oxidase 0,0053 U/ml. Catalyst solutions (0.6, 1.2, 1.8 μM) were prepared upon dilution of a mother solution (0.18 mM) in water.

Since IC_{50} values are dependent upon the screening/detection conditions, apparent kinetic rates were calculated by the equation proposed by McCord and Fridovich with k_{NBT} 5.94 x 10^4 $mol^{-1}Ls^{-1}$. The following equation was used for the caluculated values of kMcCF reported in Table 2.

$$k_{McCF} = k_{NBT} \times [NBT] / IC_{50}$$

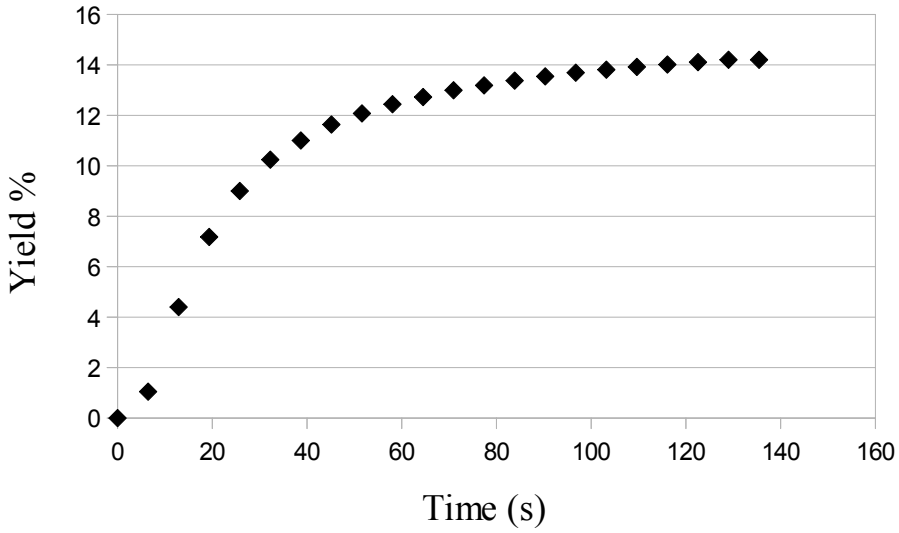

Figure. S6. H_2O_2 (33 mM) dismutation by [Mn(**3**)$(OTf)_2$] (60 μM) in 12 ml CH_3CN at 25.0 °C. Oxygen evolution was determined by GC analysis.

Table S1. Catalase-like parameters at different concentration of [Mn(**3**)$(OTf)_2$].

[Mn] concentration (μM)	Initial rate (μM O_2/min)	Endpoint (max μM O_2)	Yield O_2 (%)	TON
30	58	1467	8.9	49
60	152	1823	11.1	30
78	175	2029	12.3	26
90	191	2080	12.6	23

Conditions: [H_2O_2] = 33 mM, CH_3CN, t = 2 h, T= 25 ± 0.2 °C.

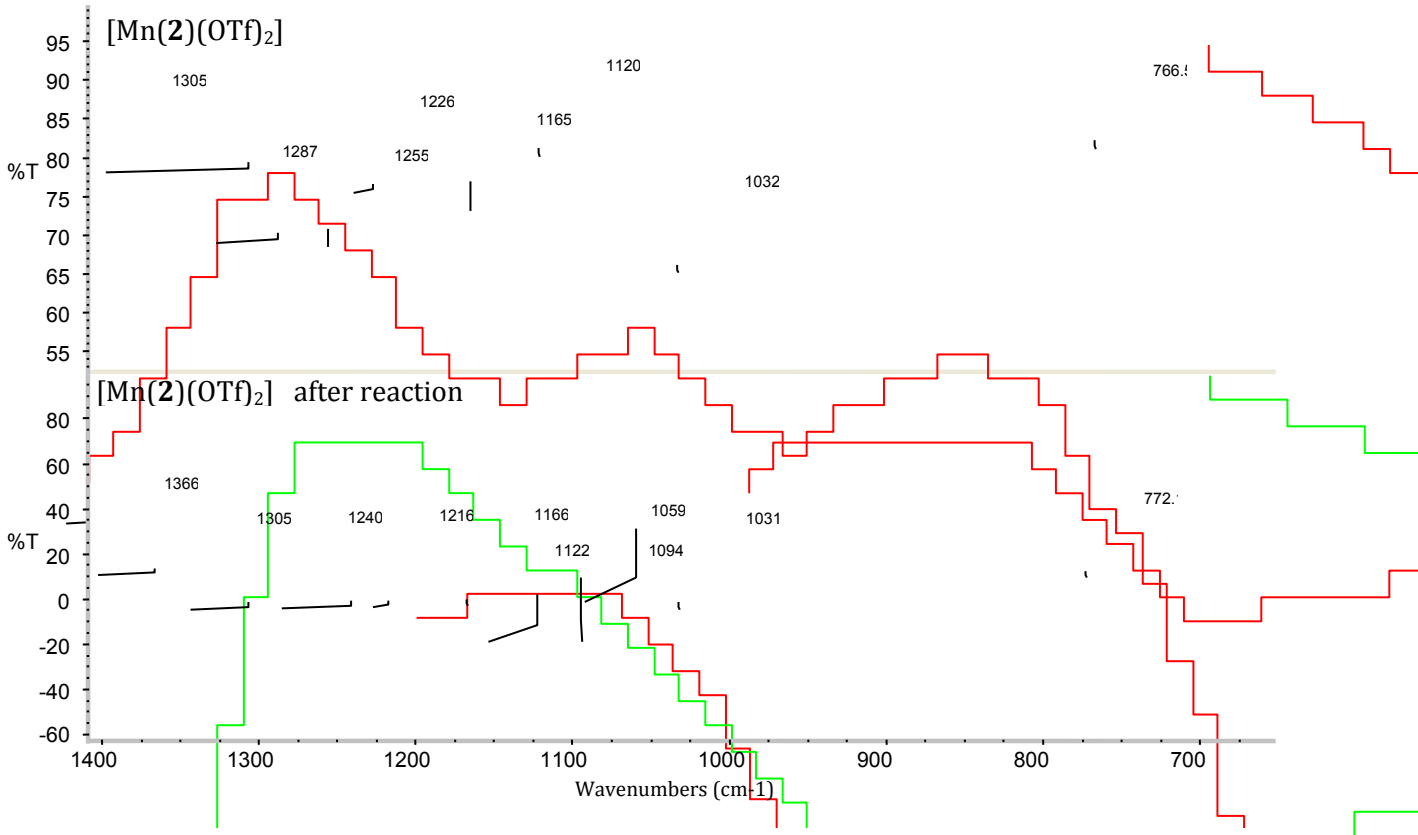

Figure S7. Comparison between spectra of [Mn(**2**)$(OTf)_2$] before/after H_2O_2 dismutation reaction: [Mn(**2**)$(OTf)_2$] 0.82 mM, H_2O_2 240 mM in 20 ml CH_3CN.

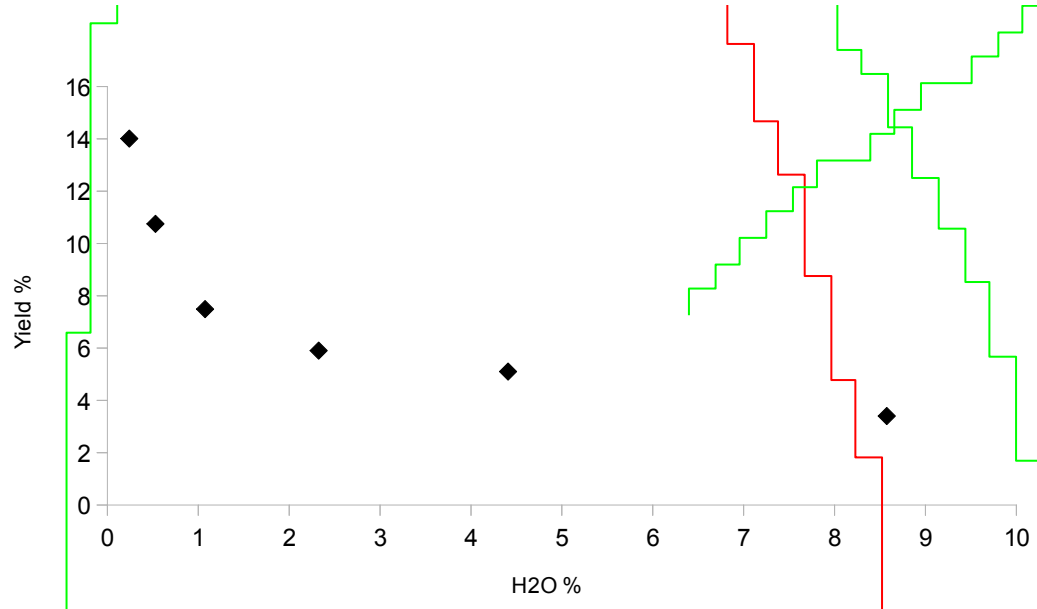

Figure S8. Inhibition of H_2O_2 (33mM) dismutation by [Mn(**3**)$(OTf)_2$] (60 μM) in CH_3CN upon addition of increasing H_2O % (v/v) at 25.0°C.

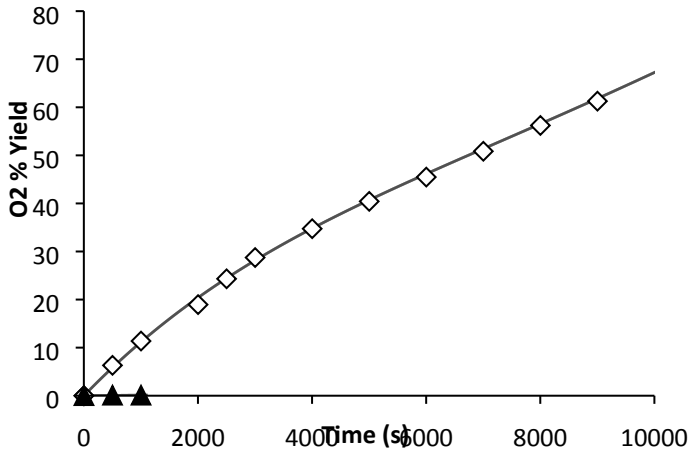

Figure S9. Yield of oxygen evolution *versus* time using [Mn(**3**)$(OTf)_2$] (60 μM), H_2O_2 33mM in CH_3CN, 25 ˚C with the addition of 10 μl NaOH 1 M ◊ and 10 μl of HCl 0.1 M ▲.

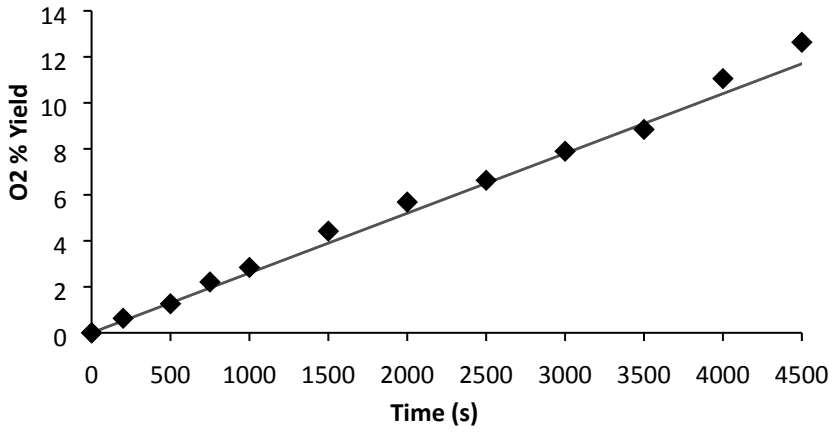

Figure S10: Evolution of oxygen versus time for [Mn(**3**)$(OTf)_2$] 60μM, imidazole 600 μM, H_2O_2 33mM, in borate buffer 50 mM pH 9.2, 25°C.

Supporting Information — X-Ray Crystallography

Crystal data for [Mn(**1**)Cl_2]: $C_{21}H_{25}Cl_2MnN_5 \cdot CH_2Cl_2$, M = 558.23, orthorhombic, *Pbca* (no. 61), a = 15.97620(17), b = 15.10805(17), c = 21.3826(2) Å, V = 5161.10(9) Å^3, Z = 8, D_c = 1.437 g cm^{-3}, μ(Mo-Kα) = 0.946 mm^{-1}, T = 173 K, colourless blocks, Oxford Diffraction Xcalibur 3S diffractometer; 9061 independent measured reflections (R_{int} = 0.0257), F^2 refinement,[8] R_1(obs) = 0.0349, wR_2(all) = 0.0976, 7581 independent observed absorption-corrected reflections [$|F_o| > 4\sigma(|F_o|)$, $2\theta_{max}$ = 66°], 342 parameters. CCDC 958982.

Crystal data for [Mn(**2**)(OTf)$_2$]: $C_{21}H_{19}F_6MnN_3O_8S_2$, M = 674.45, triclinic, *P*-1 (no. 2), *a* = 9.9713(3), *b* = 10.0552(4), *c* = 14.0070(5) Å, α = 95.426(3), β = 99.237(3), γ = 99.809(3)°, *V* = 1355.14(9) Å^3, *Z* = 2, D_c = 1.653 g cm^{-3}, μ(Mo-Kα) = 0.733 mm^{-1}, *T* = 173 K, colourless tabular needles, Oxford Diffraction Xcalibur 3S diffractometer; 8885 independent measured reflections (R_{int} = 0.0194), F^2 refinement,[8] R_1(obs) = 0.0430, wR_2(all) = 0.1200, 6948 independent observed absorption-corrected reflections [$|F_o| > 4\sigma(|F_o|)$, $2\theta_{max}$ = 66°], 436 parameters. CCDC 958983.

The X-ray crystal structure of [Mn(**1**)Cl$_2$]

The included dichloromethane solvent molecule in the structure of [Mn(**1**)Cl$_2$] was found to be severely disordered. Five orientations were identified of ca. 44, 21, 15, 14 and 6% occupancy, their geometries were optimised, the thermal parameters of adjacent atoms were restrained to be similar, and only the non-hydrogen atoms of the major occupancy orientation were refined anisotropically (the remainder were refined isotropically).

The X-ray crystal structure of [Mn(**2**)(OTf)$_2$]

Both of the coordinated triflate groups in the structure of [Mn(**2**)(OTf)$_2$] were found to be disordered. In each case two orientations were identified, of ca. 94 and 6%, and 93 and 7% occupancy for the S(30)- and S(40)- based moieties respectively. The geometries of all four orientations were optimised, the thermal parameters of adjacent atoms were restrained to be similar, and only the atoms of the major occupancy orientations were refined anisotropically (the remainder were refined isotropically).

Table S2. Selected bond lengths (Å) and angles (°).

	[Mn(**1**)Cl$_2$]	[Mn(**2**)(OTf)$_2$]	XIDNON[9]
	X = N	X = O	X = N
Mn–N(1)	2.3008(11)	2.2517(15)	2.2984(11)
Mn–X(8)/X(17)	2.4677(11), 2.4698(11)	2.3176(13), 2.3291(13)	2.3470(12), 2.3492(11)
Mn–N(11)/N(20)	2.3645(11), 2.3880(12)	2.2926(15), 2.2809(15)	2.3060(13), 2.3330(12)

Figures

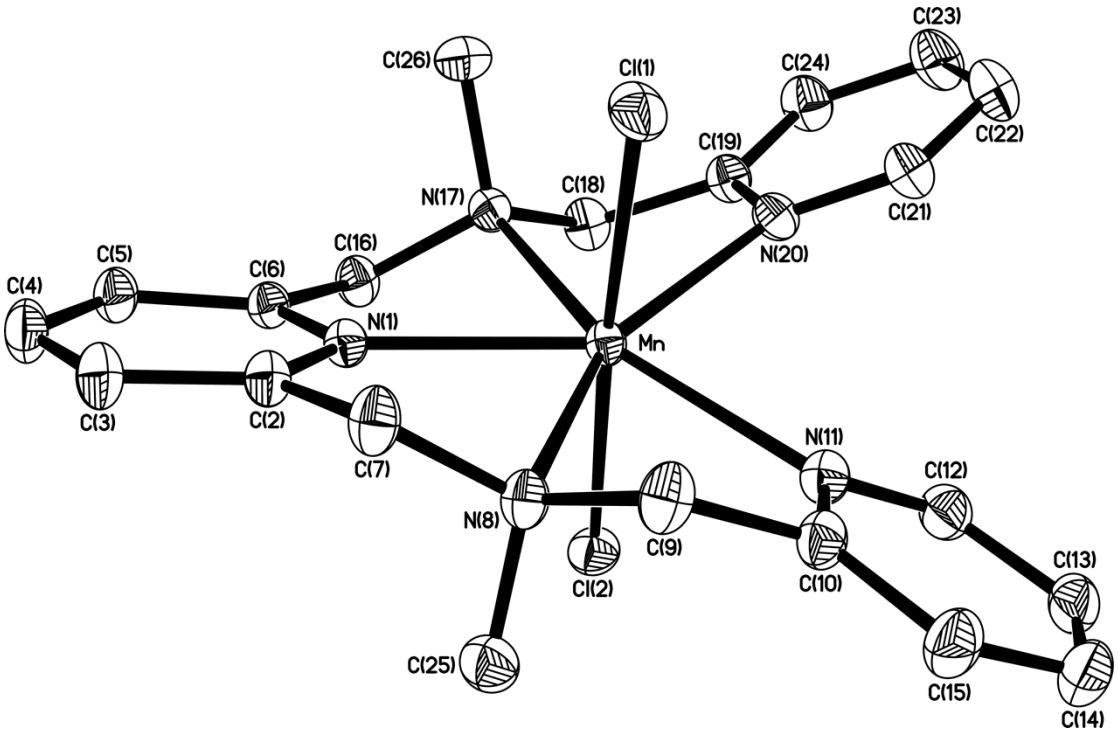

Figure S11. The crystal structure of [Mn(**1**)Cl_2] (50% probability ellipsoids).

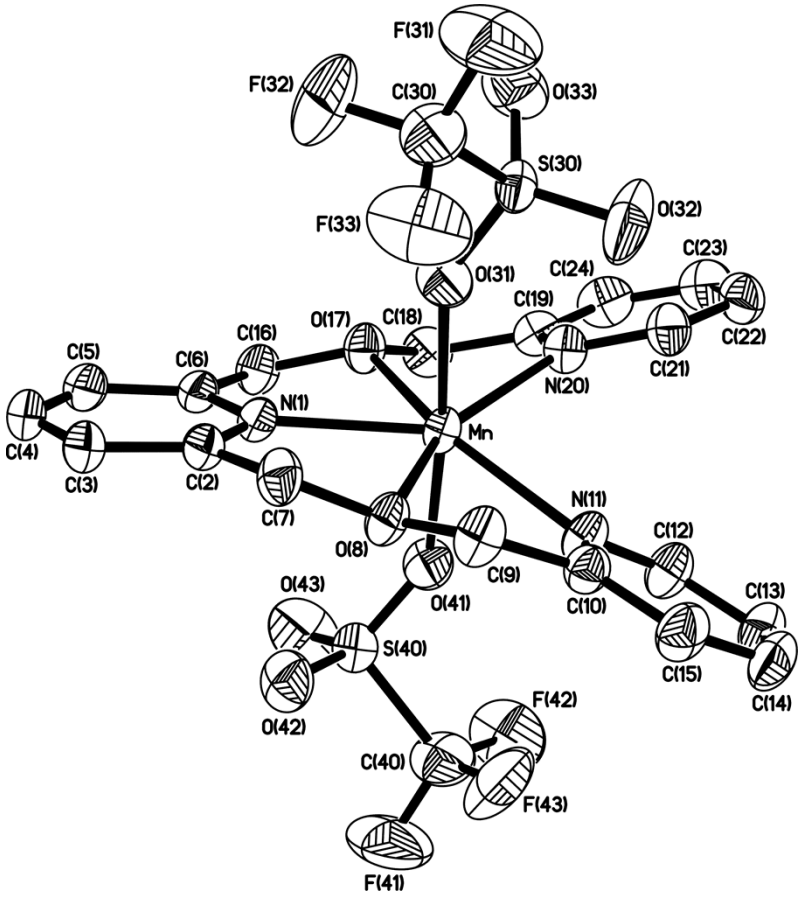

Figure S12. The crystal structure of [Mn(**2**)$(OTf)_2$] (50% probability ellipsoids).

References

1. A. Fischer, M. J. King and F. P. Robinson, *Can. J. Chem.*, 1978, **56**, 3059-3067.
2. M. Grau, J. England, R. Torres Martin de Rosales, H. S. Rzepa, A. J. P. White and G. J. P. Britovsek, *Inorg. Chem.*, 2013, **52**, 11867-11874.
3. G. R. Newkome, V. K. Gupta, F. R. Fronczek and S. Pappalardo, *Inorg. Chem.*, 1984, **23**, 2400-2408.
4. D. Jerchel and H. E. Heck, *Liebigs Ann. Chem.*, 1958, **613**, 180-184.
5. B. Nock, H.-J. Pietzsch, F. Tisato, T. Maina, P. Leibnitz, H. Spies and E. Chiotellis, *Inorg. Chim. Acta*, 2000, **304**, 26-32.
6. M. Seitz, A. Kaiser, A. Tereshchenko, C. Geiger, Y. Uematsu and O. Reiser, *Tetrahedron*, 2006, **62**, 9973-9980.
7. W. Baker, K. M. Buggle, J. F. W. McOmie and D. A. M. Watkins, *J. Chem. Soc.*, 1958, 3594-3603.
8. SHELXTL, Bruker AXS, Madison, WI; SHELX-97, G.M. Sheldrick, *Acta Cryst.*, 2008, **A64**, 112-122.
9. K. Aston, N. Rath, A. Naik, U. Slomczynska, O. F. Schall and D. P. Riley, *Inorg. Chem.*, 2001, **40**, 1779-1789.